Optimization of Polymer Electrolyte Membrane Fuel Cell Performance by Geometrical Changes

Ahmadi, Nima*⁺•; Rezazadeh, Sajad
Mechanical Engineering Department, Urmia University of Technology, Urmia, I.R. IRAN

Asgharikia, Mehdi
Mechanical Engineering Department, Elm-o-Fan University of Technology, Urmia, I.R. IRAN

Shabahangnia, Ehsan
Mechanical Engineering Department, Ferdowsi University of Mashhad, Mashhad, I.R. IRAN

ABSTRACT: *Three-dimensional computational fluid dynamics in house-code of a Polymer Electrolyte Membrane Fuel Cell (PEMFC) has been developed. The conservation equations are numerically solved using finite volume technique. One of the important goals of this research is the investigation of the variation of bipolar plates width effect on the fuel cell performance compared with the conventional model, which is highlighted in the results section with more details. Additionally, in the following, we investigated numerically and experimentally, the effect of posing the single prominence on the GDL layers in the middle of the gas channels. The results indicate the noticeable increasing in current density at the same voltages, by comparing with the base model. Also, the optimum size of the prominences is obtained from experiments and simulations. To validate the numerical procedure and experimental tests, the results compared with available experimental data which show good agreement.*

KEYWORDS: *PEMFC; Geometrical configuration; GDL prominence; CFD; Current density.*

INTRODUCTION

A very thin polymer membrane is used in PEMFC as electrolyte. PEMFC is considered as a hopeful choice of ulterior power sources. This type of fuel cells has many important advantages such as high efficiency, quiet, low operating temperature, and naive design. Nevertheless, further optimization is need before this apparatus Turns successor for fossil fuels.

Protons are traveled by a polymer electrolyte which there is amongst two porous electrodes. The extant electrodes are mold as tender films and linked to the membrane. *Grubbs* [1], In fact, used cation exchange membrane polymers in fuel cells. Among the prime electrolytes which is used in PEMFC is Nafion. *Dutta et al.* [2] presented the prior 3D model. *Berning et al.* [3],

suggested a steady-state, 3D and non-isothermal models for PEMFC. However, these systems are still not suitable for mercantile uses. One of the most important goals of recent development is focused on toll diminution and manufacturing the catalyst, membranes, and bipolar plates in high volume. This subject will come through by persistent researches to enhance performance and enlarge stack life.

Newly, some simulation and empirical tests on PEMFCs, by miscellaneous geometries is performed. *Ahmad et al.* [4] studied on the geometries with rectangular, parallelogram and trapezoidal channel configuration. The results in a skimp voltage are compared with each other. *Rezazadeh et al.* [5, 6], investigated the gas diffusion layer thickness effects on PEMFC performance. As the GDL thickness decreases, the hydrogen and oxygen paths to reach the electrochemical reaction area (anode and cathode catalyst layer respectively) decrease. It means that, the ion conductivity resistance (ohmic loss) decreases. In this way, the species reach the anode and cathode catalyst layer sooner and combines with each other faster and forms the water further. So it can be resulted that the case with lower GDL thickness has better performance. *Ahmadi et al.* [7, 8] studied the effect of parallelogram gas channel and shoulder geometry on fuel cell performance. The result of this paper indicated that the model with the parallelogram gas channel cross section has lower performance. The reason can be explained by the species distribution is not well uniformed compared with the cell with rectangular gas channel. Also they investigated the effect of prominent GDLs numerically, by posing prominence on inlet and exit region of the gas channel.

One of the main requirements of these cells is maintaining a high water content in the electrolyte to ensure high ionic conductivity. Water management has a noticeable impact on cell performance, because at high current densities mass transport issues associated with water formation and distribution limit cell output. There are other parameters, which affect cell performance such as operating temperature, pressure and humidification of the gas in the cell. *Lee et al.* [9] suggested a CFD model for simulating the PEMFC. *Kim et al.* [10] improved the performance of PEMFC. In recent years modern numerical methods presented to investigate

the performance improvement of PEMFC. *Akbari et al.* [11] used lattice –Boltzmann method to indicate the water droplet dynamic behavior. It is necessary to understand these parameter and their effects on cell performance *Carral et al.* [12] applied a finite element technique to simulate PEMFC stack. The effect of vital parameters on the PEMFC performance is studied by *Ahmadi et al.* [13]. *Kanani et al.* [14] suggested a new plan for increasing the efficiency of PEMFC. *Chen et al.* [15] investigate the thermal effect of catalyst layer by molecular dynamic method. *Yan et al.* [16] investigate the species distribution in the catalyst layer in unsteady situation. For this reasons we understand it is a point to set up these design factors at optimum values in order to increase the PEMFC operation performance. In this paper, temperature distribution for various cell voltages, major transport phenomena in conventional model of PEMFC was investigated. Also the effects of operating pressure and GDL geometrical configuration on cell performance and output cell voltage were studied. The all of numerical modeling data were validated by experimental data. To evaluate to numerical and experimental tests results, the results of base model were validated with experimental data.

MATHEMATICSL MODEL

Figs. 1 and 2 show schematic of a single cell of a PEMFC (base model).

It is made of two porous electrodes, a polymer electrolyte membrane, two-catalyst layer and two-gas distributor plates. The membrane is sandwiched between the gas channels.

Model Assumptions

The model includes some assumptions which are listed below:

● Gases mixture are assumed to be ideal gas mixture.

● The GDLs and catalyst layers are homogeneous porous media.

● The flow is incompressible and laminar while the pressure gradients and velocities are small.

Governing Equations

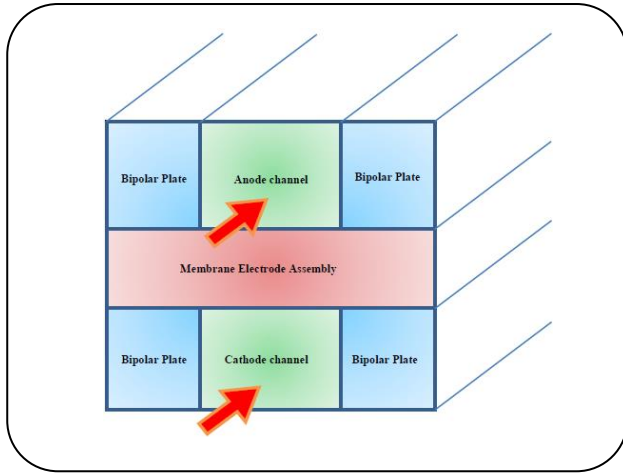In present simulation, a single domain model formulation was used for the governing equations.

Fig. 1: Schematic of a PEMFC (base case).

Fig. 2: Side view schematic of base case (Conventional model).

These governing equations consist of mass conservation, momentum, species and charge equations, which can be written as follow:

$$(\nabla.\rho u) = 0 \tag{1}$$

$$\frac{1}{\left(\varepsilon^{eff}\right)^2}\nabla.\left(\rho uu\right) = -\nabla P + \nabla.\left(\mu\nabla u\right) + S_u \tag{2}$$

$$\nabla.\left(uC_K\right) = \nabla.\left(D_K^{eff}\nabla C_K\right) + S_K \tag{3}$$

$$\nabla.\left(\kappa_e^{eff}\nabla\Phi_e\right) + S_\Phi = 0 \tag{4}$$

In Eq. (1) ρ is the density of gas mixture. According to model assumption, mass source and sink term neglected. ε is the efficient porosity entrant porous inductor, and the viscosity of the gas mixture in the momentum equation is shown as μ in Eq. (2). S_u is the momentum equation source term and is used to describe Darcy's drag for flow thru porous gas diffusion layers and catalyst layers:

$$S_u = -\frac{\mu}{K}u \tag{5}$$

K is the gas permeability in porous zones. D_K^{eff} in species equation as shown in Eq. (3), is the effective diffusion coefficient of species *k*. (e.g. hydrogen, oxygen, nitrogen and water vapor) It is defined to describe the effects of porosity in the porous gas diffusion and catalyst layers and presented as follow:

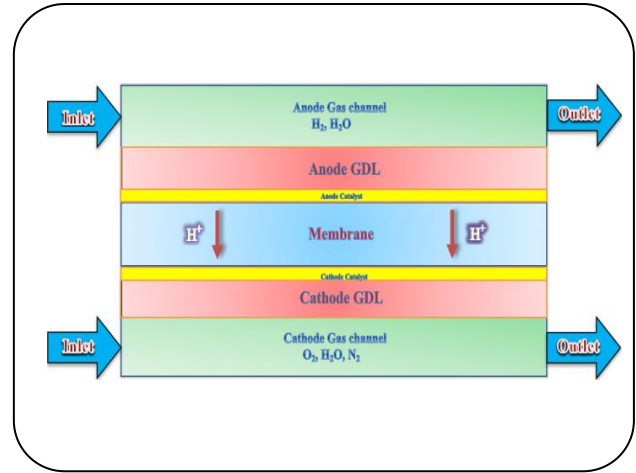$$D_K^{eff} = \left(\varepsilon^{eff}\right)^{1.5}D_K \tag{6}$$

Additionally, diffusion coefficient is function of temperature and pressure by next equation:

$$D_K = D^\circ_K\left(\frac{T}{T_\circ}\right)^{\frac{3}{2}}\left(\frac{P_\circ}{P}\right) \tag{7}$$

Transport properties for species are given in Table 1.

Charge conservation equation is shown in Eq. (4). κ_e is the ionic conductivity in the ion metric phase :

$$\kappa_e = exp\left[1268\left(\frac{1}{303} - \frac{1}{T}\right)\right]\times\left(0.005139\lambda - 0.00326\right) \tag{8}$$

Moreover, in recent equation, λ is defined as the number of water molecules per sulfonate group inside the membrane. The water content can be assumed as a function of water activity (a). It is defined as:

$$\lambda = 0.3 + 6a\left[1 - \tanh\left(a - 0.5\right)\right] + \tag{9}$$
$$3.9\sqrt{a}\left[1 + \tanh\left(\frac{a - 0.89}{0.23}\right)\right]$$

Water activity (a) is defined by:

$$a = \frac{C_w RT}{P_w^{sat}} \tag{10}$$

The proton conductivity, in the catalyst layers can be given by:

$$\kappa_e^{eff} = \varepsilon_m^{1.5}\kappa_e \tag{11}$$

Table 1: Transport properties given by Jung et al. (2007) [   ].

Property	value
H_2 Diffusivity in the gas channel, $D^0{}_{H2}$	1.10×10^{-04} m^2/s
O_2 Diffusivity in the gas channel, $D^0{}_{o2}$	3.20×10^{-05} m^2/s
H_2O Diffusivity in the gas channel, $D^0{}_{H2o}$	7.35×10^{-05} m^2/s
H_2 Diffusivity in the membrane, $D^{mem}{}_{H2}$	2.59×10^{-10} m^2/s
O_2 Diffusivity in the membrane, $D^{mem}{}_{o2}$	1.22×10^{-10} m^2/s

Table 2: Source/Sink term for conservation equations given by Jung et al. (2007) [   ].

	Momentum	species	charge
Flow channels	$S_u = 0$	$S_K = 0$	$S_\Phi = 0$
Bipolar plates	$S_u = -\dfrac{\mu}{K} u$	$S_K = 0$	$S_\Phi = 0$
GDLs	$S_u = -\dfrac{\mu}{K} u$	$S_K = 0$	$S_\Phi = 0$
Catalyst layers	$S_u = 0$	$S_K = -\nabla.\left(\dfrac{n_d}{F} I\right) - \dfrac{S_K j}{nF}$	$S_\Phi = j$
Membrane	$S_u = 0$	$S_K = -\nabla.\left(\dfrac{n_d}{F} I\right)$	$S_\Phi = 0$

In recent equation, ε_m is the volume fraction of the membrane-phase in the catalyst layer. The source and sink term in Eq. (3) and (4) are presented in Table 2.

Local current density in the membrane can be calculated by:

$$I = -\kappa_e \nabla \Phi_e \tag{12}$$

Finally, the average current density is equal to [18]:

$$I_{ave} = \frac{1}{A} \int_{A_{mem}} I\, dA \tag{13}$$

Where, *A* is the active area over the MEA.

Water transport

In PEMFCs, water molecules are transported via electro-osmotic drag due to the properties of polymer electrolyte membrane. H$^+$ transports water molecules through the polymer electrolyte membrane. This transport phenomenon is called electro-osmotic drag. In addition, the water vapor is also produced in the catalyst layers due to the oxygen reduction reaction. So the water management is very vital fact in fuel cell subject.

In the polymer electrolyte membrane water transportation is given by *Seddiq et al.* [19]:

$$\nabla.\left(D^{mem}_{H_2O} \nabla C^{mem}_{H_2O}\right) - \nabla.\left(\frac{n_d}{F} i\right) = 0 \tag{14}$$

Where n_d and $D^{mem}_{H_2O}$ are defined as drag coefficient of water and the diffusion coefficient of water in the membrane phase, respectively.

The number of water molecules transported by each H$^+$ is called the water drag coefficient. It can be determined from the following equation:

$$n_d = \begin{cases} 1 & \lambda < 9 \\ 0.117\lambda - 0.0544 & \lambda \geq 9 \end{cases} \tag{15}$$

The diffusion coefficient of water in the polymer membrane is dependent on the water content of the membrane. It is obtained by the following experimental expression:

$$D_W^{mem} = \tag{16}$$

$$\begin{cases} 3.1 \times 10^{-7} \lambda \left(e^{0.28\lambda} - 1\right) e^{\left(\frac{-2346}{T}\right)} & 0 < \lambda \le 3 \\ 4.17 \times 10^{-8} \left(1 + 161 e^{-\lambda}\right) e^{\left(\frac{-2346}{T}\right)} & \text{Otherwise} \end{cases}$$

The transfer currents or source terms are non-zero only inside the catalyst layers. The transfer current at anode and cathode can be described by Tafel equations as follows:

$$R_{an} = j_{an}^{ref} \left(\frac{[H_2]}{[H_2]_{ref}}\right)^{\gamma an} \left(e^{\alpha_{am}F\eta_{an}/RT} - e^{-\alpha_{cat}F\eta^{an}/RT}\right) \tag{17}$$

$$R_{cat} = j_{cat}^{ref} \left(\frac{[O_2]}{[O_2]_{ref}}\right)^{\gamma cat} \left(-e^{\alpha_{am}F\eta_{cat}/RT} + e^{-\alpha_{cat}F\eta^{cat}/RT}\right) \tag{18}$$

According to the Tafel equation, the current densities in the anode and cathode catalysts can be expressed by the exchange current density, reactant concentration, temperature and over-potentials. Hence, the surface over potential is defined as the difference between proton potential and electron potential.

$$\eta_{an} = \phi_{sol} - \phi_{mem} \tag{19}$$

$$\eta_{cat} = \varphi_{sol} - \varphi_{mem} - V_{oc} \tag{20}$$

The open circuit potential at the anode is assumed to be zero. Also, the open circuit potential at the cathode becomes a function of a temperature. So we have the following equation from experimental finding:

$$V_{oc} = 0.0025T + 0.2329 \tag{21}$$

The membrane protonic conductivity is dependent on water content. Therefore, σ_m is the ionic conductivity in the ionomeric phase:

$$\sigma_m = (0.005139\lambda - 0.00326) \exp\left[1268\left(\frac{1}{303} - \frac{1}{T}\right)\right] \tag{22}$$

Energy equation given by Eq. (23):

$$\nabla \cdot (\rho \mathbf{u} T) = \nabla \cdot (\lambda_{eff} \nabla T) + s_T \tag{23}$$

In last expression, λ_{eff} is the effective thermal conductivity. S_T is the source term of energy equation and defined with the following equation:

$$S_T = I^2 R_{ohm} + h_{reaction} + \eta_a i_a + \eta_c i_c \tag{24}$$

In above equation, R_{ohm}, is the membrane ohmic resistance. $h_{reaction}$, is the heat produced via chemical reactions. Anode and cathode overpotentials are presented by η_a and η_c:

$$R_{ohm} = \frac{t_m}{\sigma_e} \tag{25}$$

t_m is the membrane thickness.

$$\eta_a = \frac{RT}{\alpha_a F} \ln\left[\frac{IP}{j_{0_a} P_{0_{H_2}}}\right] \tag{26}$$

$$\eta_C = \frac{RT}{\alpha_c F} \ln\left[\frac{IP}{j_{0_c} P_{0_{O_2}}}\right] \tag{27}$$

Where, α_a and, α_c are the anode and cathode conduction modulus. $P_{0_{H_2}}$, $P_{0_{O_2}}$ are sectorial pressure of hydrogen and oxygen respectively and j_0 is the reference exchange current density.

The fuel and oxidant fuel rate u is given by following equations:

$$u_{in,a} = \frac{\xi_a I_{ref} A_{mem}}{2C_{H_2,in} F A_{ch}} \tag{28}$$

$$u_{in,c} = \frac{\xi_c I_{ref} A_{mem}}{4C_{O_2,in} F A_{ch}}$$

In present equation, I_{ref} and ξ are the reference current density and stoichiometric ratio, respectively. ξ is distinguished as the proportion among the quantity supplied and the quantity required of the fuel based on the reference current density. The species concentrations of flow inlets are assigned by the humidification conditions of both the anode and cathode inlets.

Boundary condition

Eqs. (1) to (4) form the complete set of governing equations for the traditional mathematical model. Boundary conditions are expressed in Table 3 in more details.

Table 3: Boundary condition of fuel cell.

Type of boundary condition	Place in the fuel cell geometry
$u=u_{in}$, $T=T_{in}$, $v=0$, $C_{H_2}=C^a_{H_{2,in}}$, $C_{H_2O}=C^a_{H_{2O,in}}$	Anode channel inlet
$u=u_{in}$, $T=T_{in}$, $v=0$, $C_{O_2}=C^c_{O_{2,in}}$, $C_{N_2}=C^c_{N_{2,in}}$	Cathode channel inlet
$\dfrac{\partial u}{\partial x}=\dfrac{\partial v}{\partial x}=\dfrac{\partial w}{\partial z}=\dfrac{\partial T}{\partial x}=0$	Anode and Cathode channel outlet
$\left.\dfrac{\partial u}{\partial y}\right\|_{y=h_1^-}=\varepsilon_{eff,GDL}\left.\dfrac{\partial u}{\partial y}\right\|_{y=h_1^+}$, $\left.\dfrac{\partial v}{\partial y}\right\|_{y=h_1^-}=\varepsilon_{eff,GDL}\left.\dfrac{\partial v}{\partial y}\right\|_{y=h_1^+}$	Interface of gas channel and GDLs
$\varepsilon_{eff,GDL}\left.\dfrac{\partial u}{\partial y}\right\|_{y=h_2^-}=\varepsilon_{eff,GDL}\left.\dfrac{\partial u}{\partial y}\right\|_{y=h_2^+}$, $\varepsilon_{eff,GDL}\left.\dfrac{\partial v}{\partial y}\right\|_{y=h_2^-}=\varepsilon_{eff,GDL}\left.\dfrac{\partial v}{\partial y}\right\|_{y=h_2^+}$ $\varepsilon_{eff,GDL}\left.\dfrac{\partial w}{\partial y}\right\|_{y=h_2^-}=\varepsilon_{eff,GDL}\left.\dfrac{\partial w}{\partial y}\right\|_{y=h_2^+}$	Interface of GDLs and catalyst layers
$U=v=w=C_i=0$	Interface of catalyst layers and membrane
$u=v=w=C_i=0$, $T_{surface}=353\ K$	Upper surface of channels
$u=w=0$, $T_{surface}=T_{wall}$	Lower surface of gas channel
$\phi_{sol}=0$, $\dfrac{\partial\phi_{mem}}{\partial y}=0$	Upper surface of anode bipolar plate
$\dfrac{\partial\phi_{mem}}{\partial x}=0$, $\dfrac{\partial\phi_{mem}}{\partial z}=0$, $\dfrac{\partial\phi_{sol}}{\partial x}=0$, $\dfrac{\partial\phi_{sol}}{\partial z}=0$	External surface

RESULTS AND DISCUSSION

Numerical and experimental procedure

To solve governing equations numerically with related initial and boundary condition, the implicit finite volume method is used to discretize the partial derivatives. The SIMPLE algorithm was adopted for the pressure correction equation. Iterative methods were used to solve resultant algebraic equations. The calculations are repeated in each time step until the convergence criterion is met. The convergence criterion reads as the relative error to be less than 10^{-9}. Also a series of empirical tests were performed to validate the numerical results. These experimental tests consist applied for base model, pressure increasing effect and for prominent GDLs, separately. Also in order to validating both of the numerical and experimental results for base model, these results have compared with *Wang et al.* (2003) experimental data. It is shown in Fig. 3a. As can be seen, a favorable agreement between them.

Structured meshes are applied for base model and the finer meshes were chosen for reacting area such as membrane and catalyst layers. Grid independence test was indicated the optimum number of meshes (174 000) (Fig. 3b). The number of iterations was determined as 1500 and 6000 for low and high current density respectively. An IBM-PC-Pentium 4 (CPU speed is 2.4 GHz) was used to solve the set of equations. The computational time for solving the set of equations was 12 h. Fuel cell
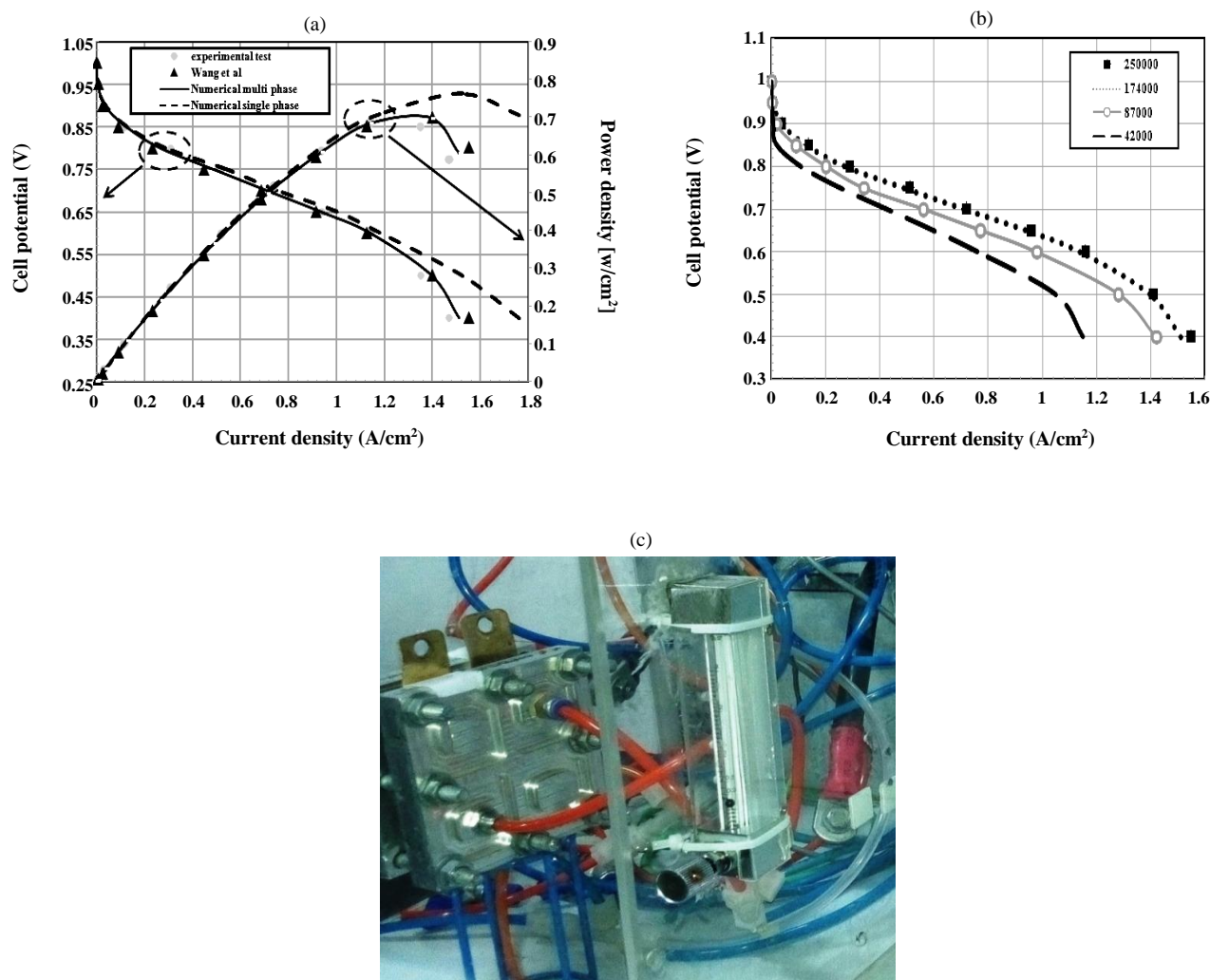
Fig. 3: a) Polarization curve of numerical model and experimental data and power density curve at 1.5 (A/m²).
b) Grid independency polarization curve. c) Experimental setup.

operational situation and geometrical parameters are shown in Table 4. Fig. 3 presents the experimental setup in more details.

Results of base model

Fig. 4 Indicates that at cathode side, water amount is growing up along the flow direction. This fact is the result of two important phenomena: water establishment in cathode catalyst layer and water transferring because of drag from anode to cathode. More water presence at the exit region of fuel cell cools the cell and decreases the temperature.

Water molecules in the inlet of the anode gas channel are portaged mostly to the cathode by electro-osmotic drag but the electro-osmotic mass flux enhances along the channel. As shown in Fig. 5, rate of the back diffusion is too shorter than the electro-osmotic mass flux. Therefore the genuine water mass amidst the membrane is propelled from anode to cathode side.

In addition, the water in the anode catalyst layer is accountable for bearing the hydrogen protons to the cathode. So its value should be reduced along the flow direction from inlet to outlet (Fig. 6). Accordingly the oxygen magnitude in the linear orientation diminishes and the water amount increases, more H^+ should be transported by water molecules. The lower the cell voltages the more water molecules transfer from anode to cathode.

Table 4: Geometrical parameters and operating conditions (Wang et al. (2003)) [   ].

Parameter	value
Gas channel length	7.0×10^{-2} m
Gas channel width and depth	1.0×10^{-3} m
Bipolar plate width	5.0×10^{-4} m
Gas diffusion layer thickness	3.0×10^{-4} m
Catalyst layer thickness	1.29×10^{-5} m
Membrane thickness	1.08×10^{-4} m
Cell temperature	343.15 K
Anode pressure	303975Pa
Cathode pressure	303975Pa
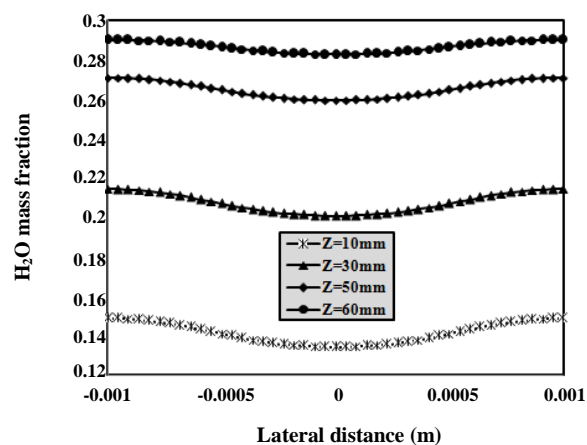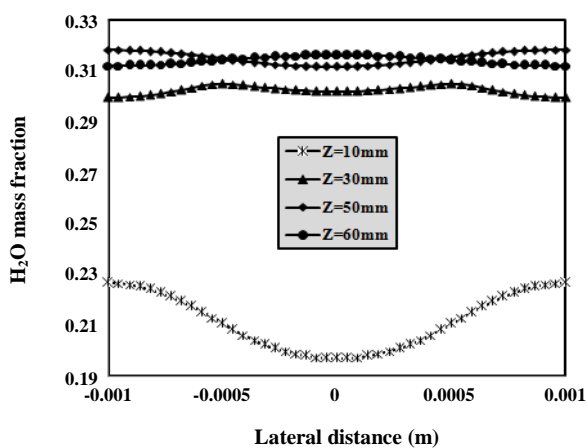
Fig. 4: Water distribution in cathode side.
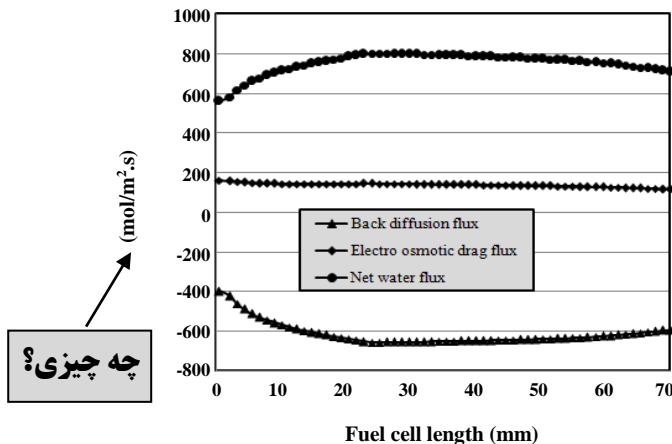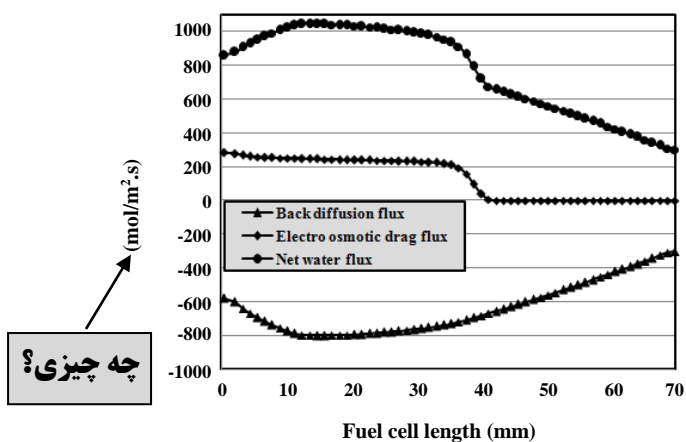
Fig. 5: Water flux along the fuel cell.
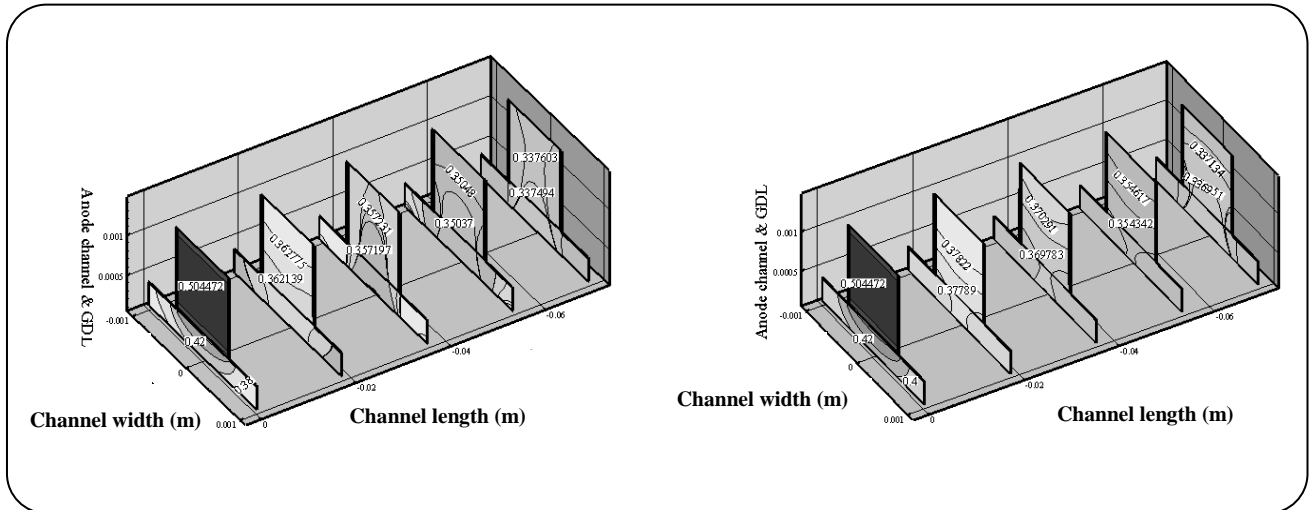
Fig. 6: Anode side water distribution at different planes of channel and GDL.
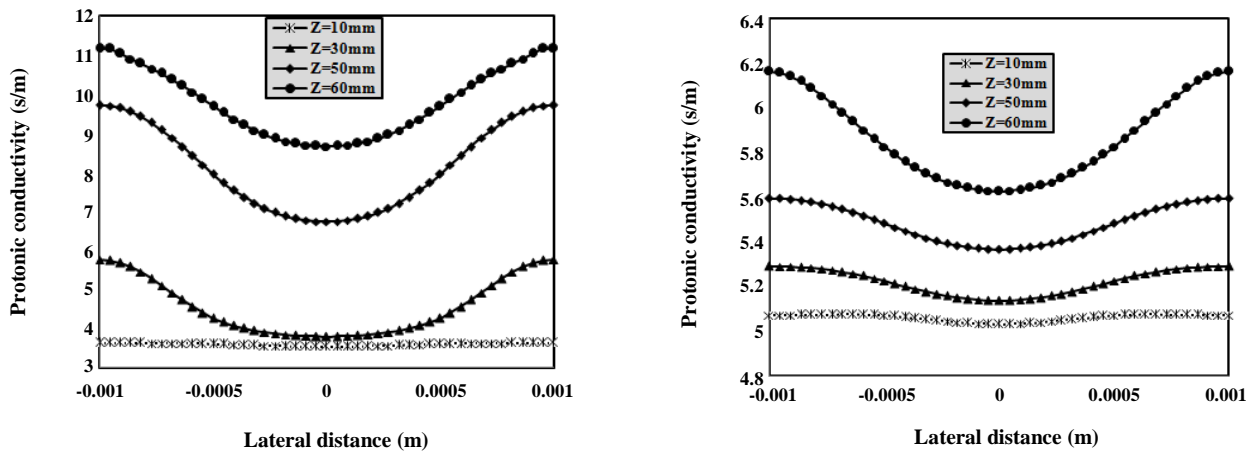
Fig. 6: Protonic conductivity at anode catalyst layer and membrane interface.

The governing parameters of the fuel cell are extremely attached on each other. One of these important parameters is membrane protonic conductivity. This operant is exorbitance associate on temperature (inversely) and water activity of anode (directly). So its magnitude at shoulder region is higher than channel region (Fig. 7).

Fig. 8 illustrates the current density distribution at the interface of cathode catalyst layer and membrane. Current density indeed is electron flux in the cell and while electrons flow through the solid phase (solid phase of gas diffusion and catalyst layers), they want to traverse the shortest path to achieve the bipolar plates. So its value is higher at the shoulder region. In addition, current density

amount dwindles along the flow direction. As it is mentioned before, water increasing along the cathode catalyst (especially at low voltages or high current densities) blocks the holes of porous zones and as a result stops the oxygen attaining to the reaction area. This fact leads to current density reduction along the flow direction.

Fig. 9 illustrate oxygen mole fraction along the cathode catalyst for two different voltages.

As can be seen on Fig. 10, the maximum temperature is in the voltage 0.4V.This is due to high reaction rate in fuel cell. Voltage gradually decreases with increasing reaction rate and maximum cell temperature reduces. Although the temperature is high relative to high voltages,
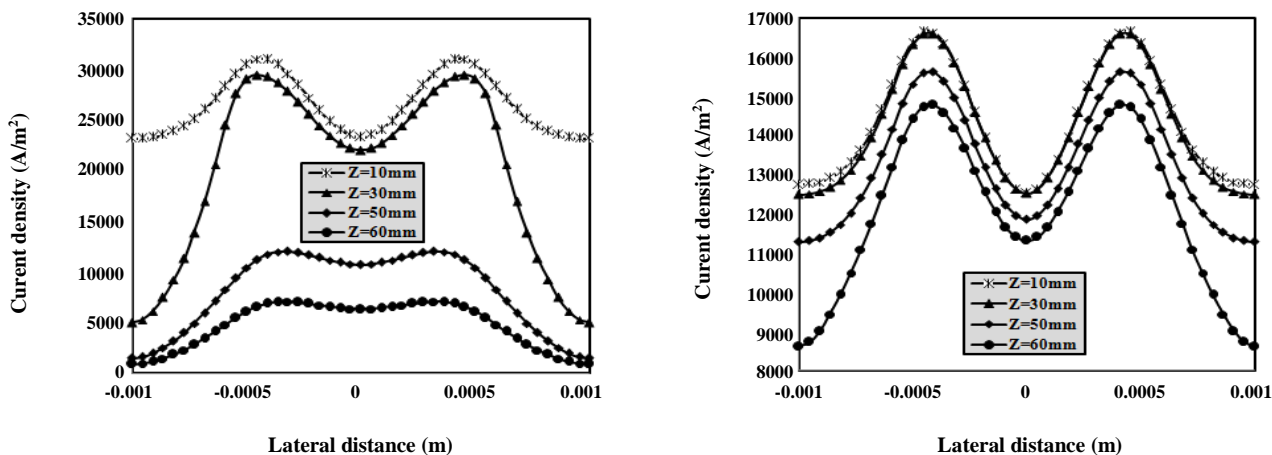
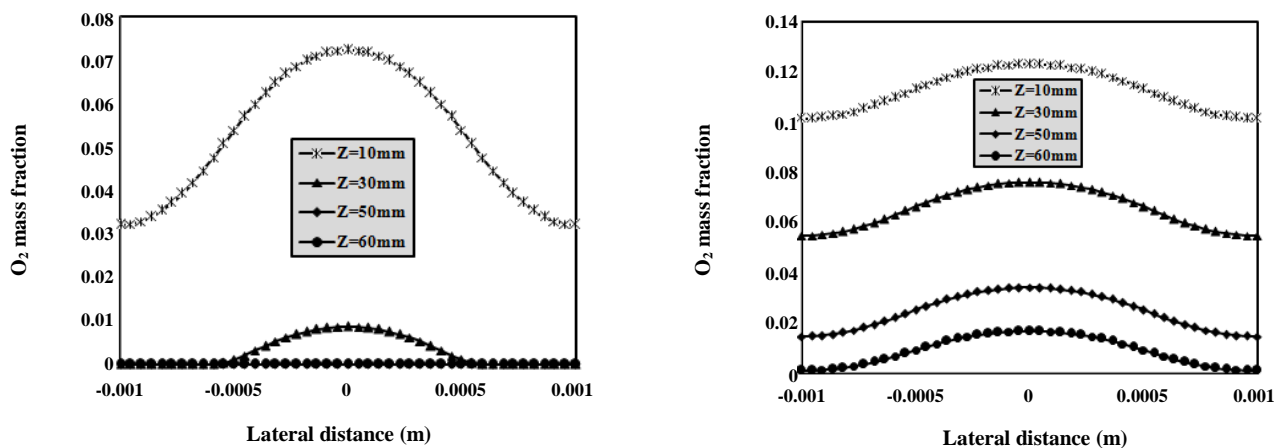*Fig. 7: Current density magnitude at cathode catalyst later and membrane interface.*

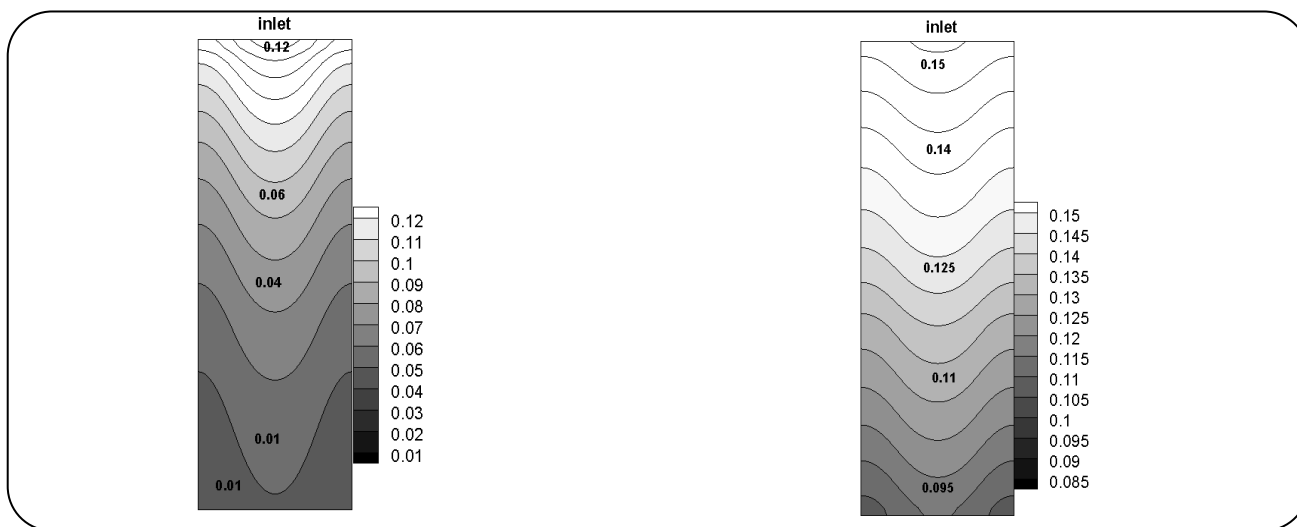*Fig. 8: Oxygen mass fraction at cathode catalyst layer and membrane interface.*

Fig. 9: Oxygen mole fraction at cathode catalyst layer and membrane interface.

Table 5: Cell geometry conditions.

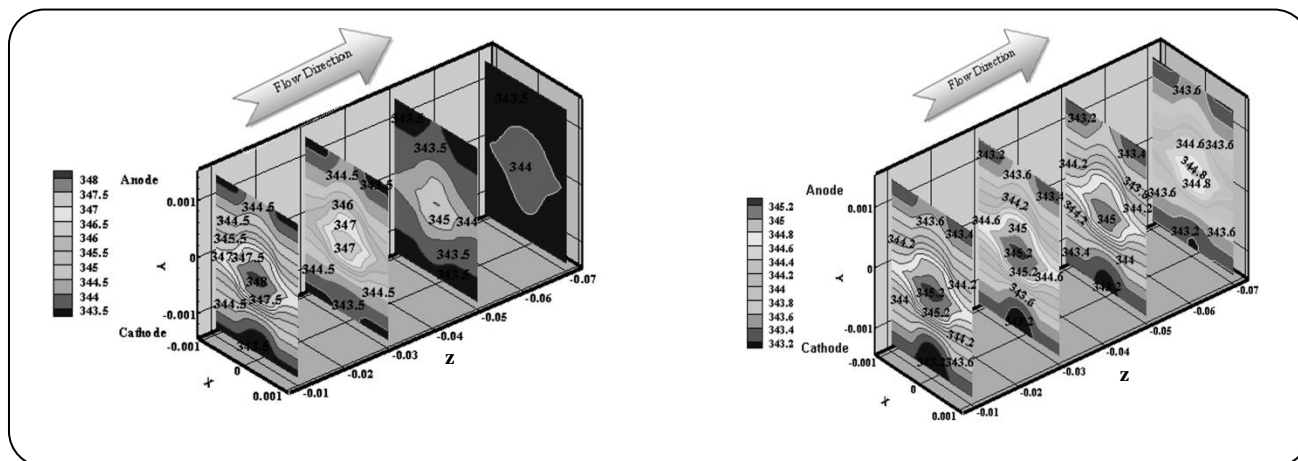| Bipolar width (mm)	Channel width (mm)	Reaction area (mm^2)	Aspect ratio
b=0.5	a=1	140	a/b=2
b=0.4	a=1	126	a/b=2.5
b=0.3	a=1	112	a/b=3.33
b=0.2	a=1	98	a/b=5
b=0.1	a=1	84	a/b=10

Fig. 10: Temperature distribution in the cell.

but at the exit region of the cell at same voltage temperature shows more severe losses. The reason can be explained as rather amount of water output in these voltages. The high rate of water production along the cell assists cooling of the cell especially at exit region of the cell. Hence, high temperature losses will happen in this voltage. At high voltage the temperature is almost constant.

Effect of channel aspect ratio on PEMFC performance

The proposed model is the cell, with different aspect ratio of channel-bipolar width. In this case the electrochemical reaction area would be changed but the boundary conditions are same with the conventional cell with straight channels (base model).

Fig. 11 shows the proposed model. It should be Saied that the comparison between the base and the other models has been done in V=0.4[V] and at interface of cathode catalyst and membrane, since significant diversity disclose themselves at underneath voltages.

Table 5 shows the geometric properties for all models. As it is clear, the channel width kept fixed and the bipolar width has been varied to achieve the better one in point view of performance.
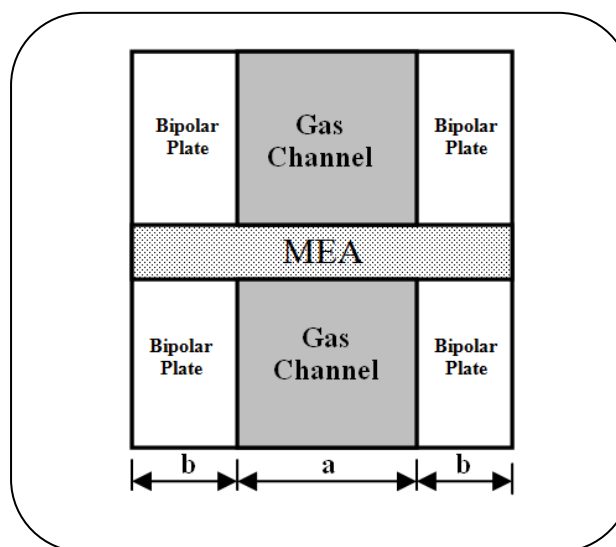

Fig. 11: Schematic of model.

The Figs. 12 a, b illustrate the numerical and experimental results of bipolar plates width variation effect on current density for different voltages.

At first the current density of models is presented in Fig. 13, in the interface of cathode catalyst and membrane in V=0.4[V]. By decreasing the bipolar plates width or

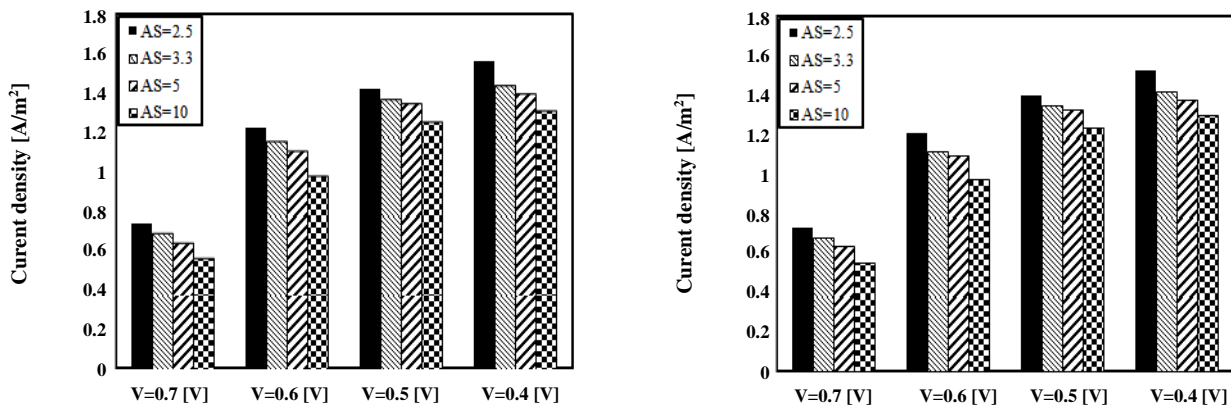*Fig. 12: Numerical (a) and experimental (b) results of bipolar plates width variation effect on current density for different voltages.*
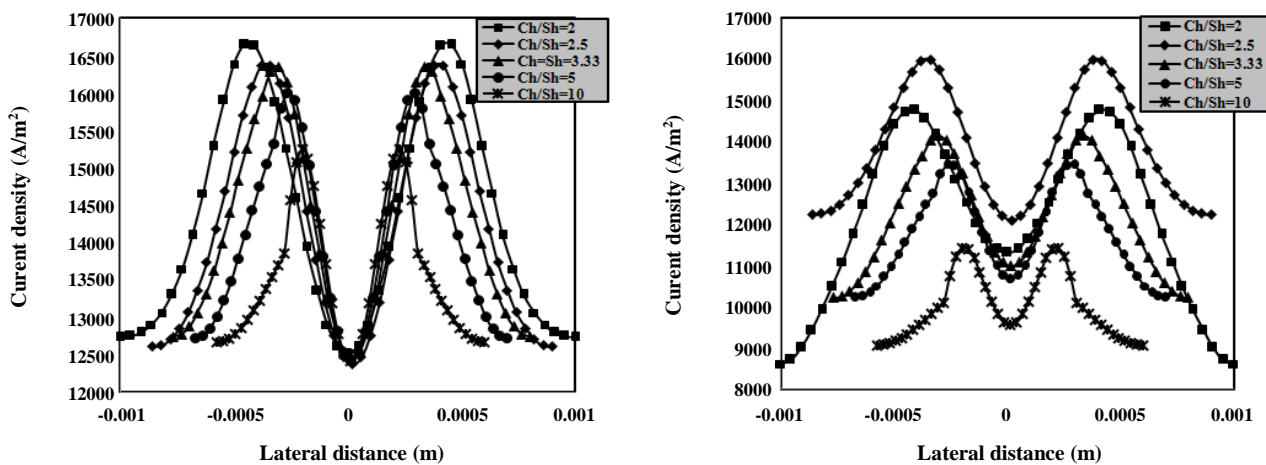

Fig. 13: Comparison of the current density of models in inlet(a), outlet (b).

increasing the aspect ratio, the current density and performance step down unless the model a/b=2.5. It means that, by decreasing b=0.5 to b=0.4 performance enhances but for b=0.3, 0.2 and 0.1 is vice versa. So there is a optimum model (when b=0.4).

Figs. 14 and 15 illustrate the cathode over potential and voltage losses. While decreasing the bipolar width, the reaction area and losses diminish. Decreasing the reaction area leads to dwindle the current density. On the other hand, decreasing the voltage losses is favorable.

The kind of current density and voltage losses distribution, can justify the species distributions (Figs. 16 and 17).

The temperature distribution is related to water amount. If there is more water the cooling will be better. Fig. 18 shows this effect clearly.

Effect of GDLs geometrical configuration

Fig. 19 shows the GDLs prominences configuration clearly at side view schematic of PEMFC. To study the performance enhancement of base model we posed a single circular prominence on GDL layers in both cathode and anode side. Thus, set of empirical tests was performed to study the effect of this geometrical change. Also by using of CFD (finite volume method) a 3-D in-house code was developed. To evaluate the results experimental and numerical results compared to each other which show good agreement. Also to study the effect of prominent GDLs, both numerical and empirical results for base model and prominent case was compared (Fig. 20). Table 6 illustrates the geometrical properties of prominent GDLs.
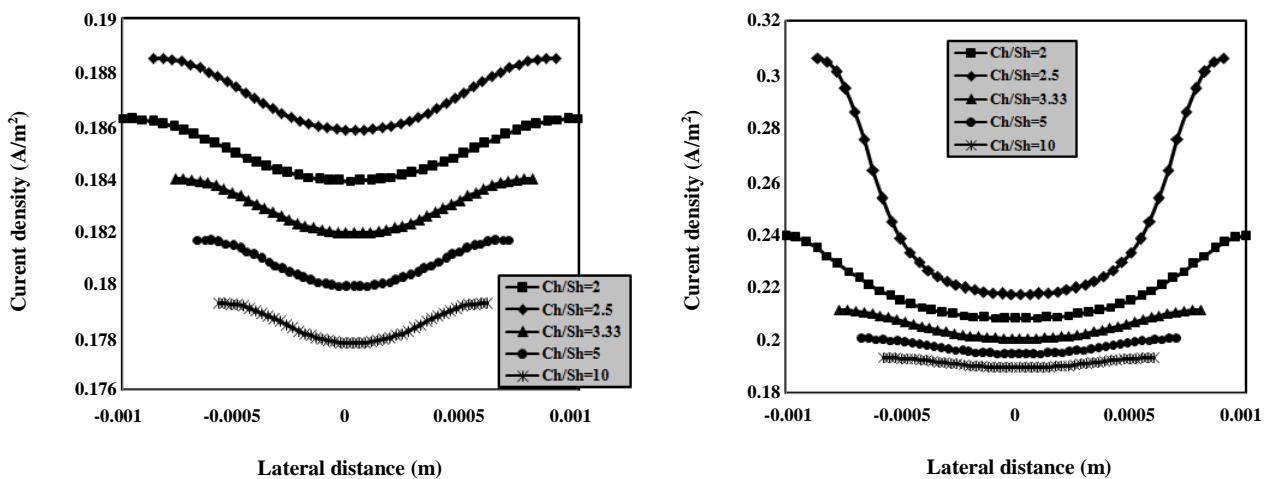
Fig. 14: Comparison of the cathode over potential in inlet(a) , outlet (b).
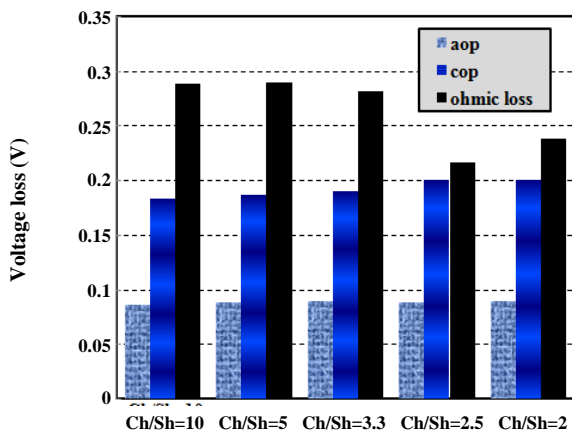

Fig. 15: Comparison of the voltage losses for proposed models.

It is clear that, GDLs with prominences produce more current density than base model at the same operating condition because it yields a notable increase in velocity by decreasing the cross sectional area of gas flow at gas channels. This leads to more supplying of the reactant gases to the catalyst layers. Thus the efficiency of catalytic reaction enhances. On the other hand, the interface of GDLs and reactant gases grows to and later reactants distribute to catalyst layers better than base model. By growing up the performance of fuel cell, consuming the oxygen at cathode side increases too. To investigate the effect of prominences in more detail the empirical test and numerical simulations are repeated for four cases (As mentioned in Table 4). It is clear that

increasing the height of prominence from 0.25mm to 0.35 yields notable enhancement in current density magnitude, in same condition. But when the prominences height is growth from 0.35mm to 0.45mm the current density magnitude which cell produces is decreased obviously. Also if the height increasing the prominences continues (From 0.45mm to 0.55mm), the current density magnitude is reduced more than before. This phenomenon is took place because of the impressing the reactant gas flow in the channel by height of the prominences. When the height of these prominences increases is a bit more than before, it is like an obstacle placed in front of the gas flow and dominates the velocity of flow and its diffusion to the reaction area. As it is seen, once the prominence height is enhance to 0.55mm the current density produced by cell is reduced more than base case.

Fig. 21 illustrates the average magnitude of oxygen mole fraction. The comparison has been made up at the interface of cathode catalyst and membrane along the cell (at 0.6 V). As depicted, in case 2 the magnitude of oxygen due to high consumption of it, reaches near zero. Against case 4, which produces less magnitude of current density, consumes less magnitude of oxygen due to diffusion problems as mentioned before.

Fig. 22 compares the voltage losses for all cases at same voltages (0.6 V) along the cell at the interface of cathode catalyst layer and membrane. To make any considerable differences to find out in cell performances with these cases, average magnitude of three main losses:
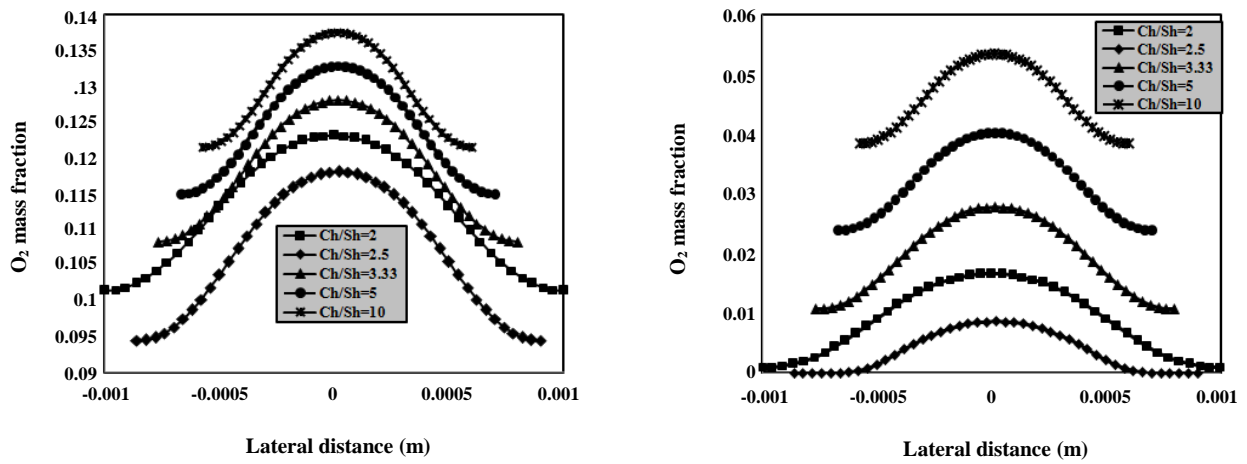
101

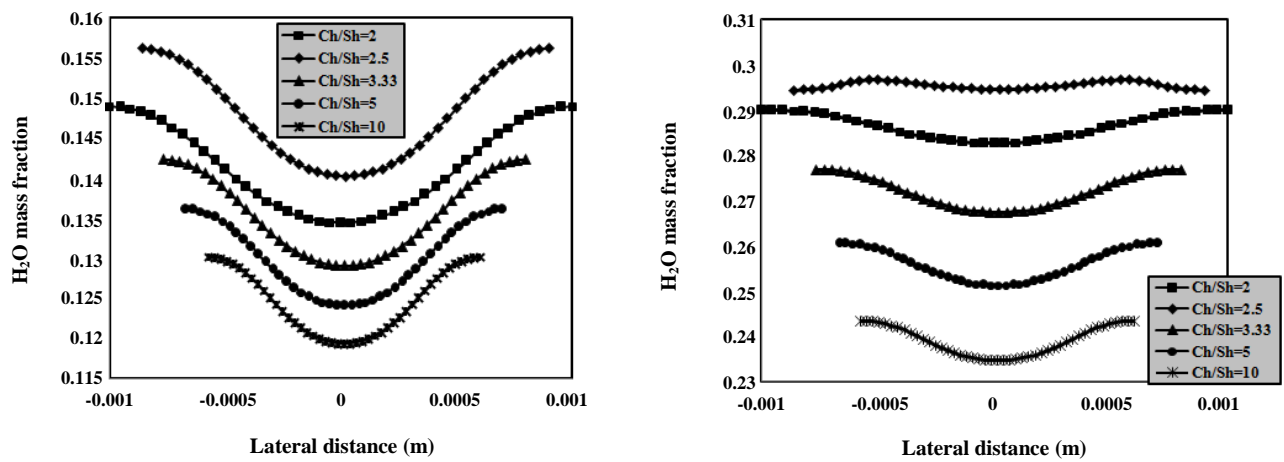*Fig. 16: Comparison of the O₂ mass fraction in inlet(a) , outlet (b).*

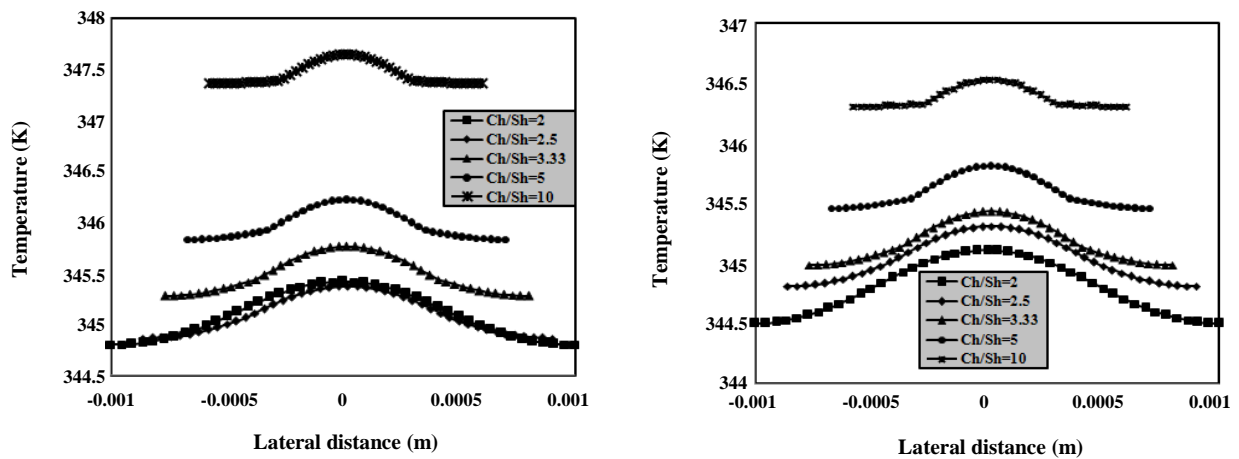*Fig. 17: Comparison of the H₂O mass fraction in inlet(a) , outlet (b).*

Fig. 18: Comparison of the temperature distribution in inlet(a) , outlet (b).

Table 6: Geometrical specification of case with prominent GDLs.

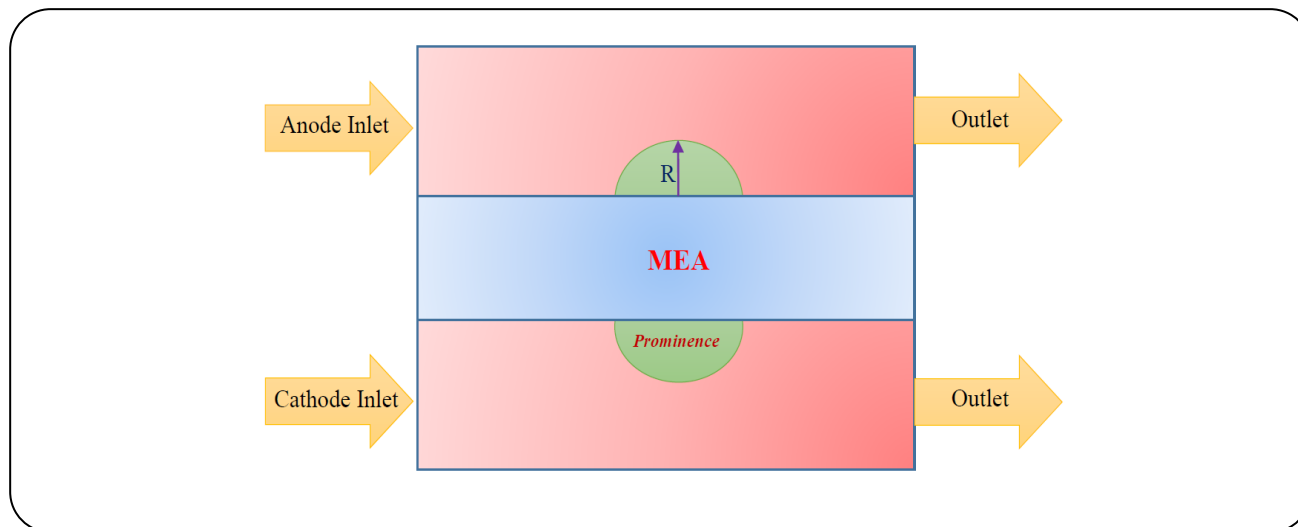| Symbol	Case 1	Case 2	Case 3	Case 4
R	0.25mm	0.35mm	0.45mm	0.55mm

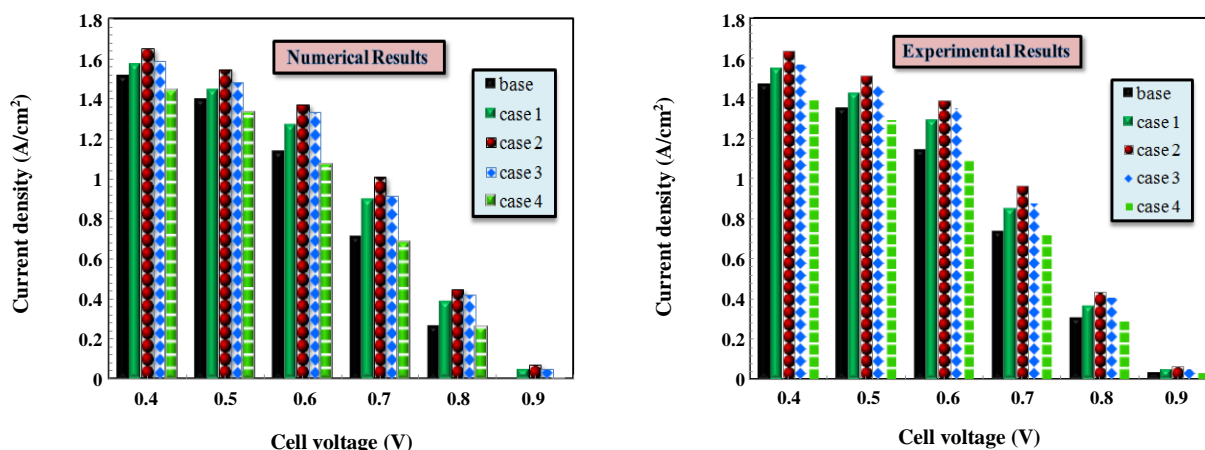*Fig. 19: Side view schematic of GDLs prominences on PEMFC.*

Fig. 20: Polarization and Power density curves for cases (numerical and experimental results).

aop (anode overpotential) cop (cathode overpotential) and ohmic loss are going to be compared. As the figures show, the value of aop for all cases is negligible. The cop and ohmic loss are account for the paramount reason for total losses.

Fig. 23 shows the comparison of the average magnitude of current density at the interface of cathode catalyst-membrane. As can be seen case 2 and case 4 have the maximum and minimum value of current density respectively.

CONCLUSIONS

In this article, series of experimental test was performed also a three dimensional computational fluid dynamics model PEMFC with straight flow channels has been simulated. The specification and performance of base model such as polarization curve, species and temperature distribution were studied. The numerical results show that, at low cell voltages (for example 0.4 V), the cell has maximum temperature which is due to high reaction rate in fuel cell.
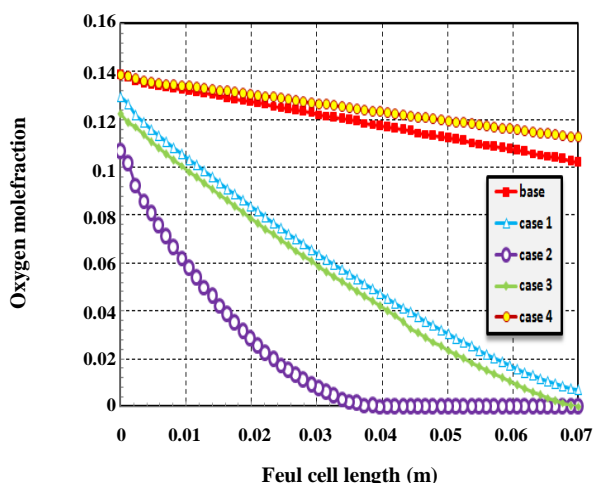
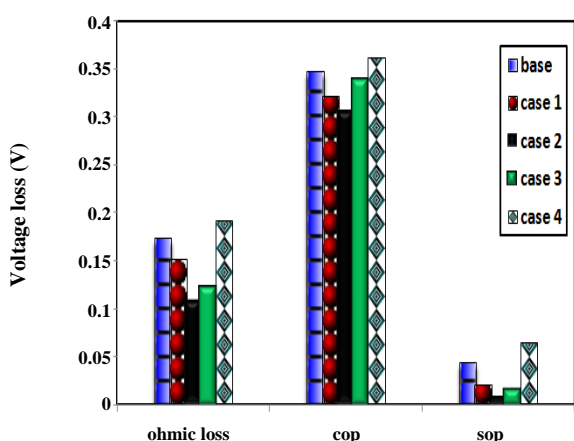**Fig. 21: Comparison the magnitude of oxygen mole fraction.**

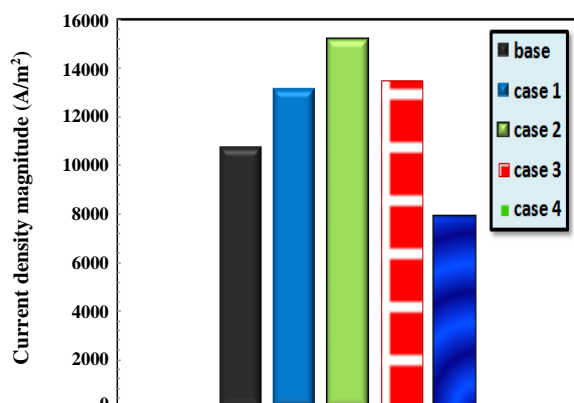**Fig. 22: Comparison the average magnitude of voltage losses.**

Fig. 23: Comparison the current flux density for two cases.

Voltage gradually decreases with increasing the reaction rate and consequently, the maximum cell temperature grows up. Meanwhile, the results reveal that these important operating parameters are highly dependent to each other and the fuel cell efficiency is under the influence by the type of species repartition. Thus, for peculiar uses in eligible voltages, for preventing from the unwilling losses, these numerical results can be useful. The important goal of this research is the investigation of bipolar plate's width variation effect on performance and species distribution. It has been concluded that there is an optimum aspect ratio which is a/b=2.5.

Additionally, the effect of GDLs geometrical configuration has been perused and observed that the case with prominent GDLs yields a remarkable increase in current density. The juncture of GDLs and reactant gases increase and later reactants penetrate to catalyst layers better than base model. The experiments and simulations were performed for different size of prominences. As can be seen the optimum size of prominence is obtained from case 2. Ultimately prominences of GDLs improve the flow of the reaction hence reduces the membrane drawing effect, therefore PEMFC performance improves.

Nomenclature

a	Water activity
C	Molar concentration, mol/m^3
D	Mass diffusion coefficient, m^2/s
F	Faraday constant, C/mol
I	Local current density, A/m^2
J	Exchange current density, A/m^2
K	Permeability, m^2
M	Molecular mass, kg/mol
n_d	Electro-osmotic drag coefficient
P	Pressure, Pa
R	Universal gas constant, J/mol K
T	Temperature, K
t	Thickness
u	Velocity vector
V_{cell}	Cell voltage
V_{oc}	Open-circuit voltage
W	Width
X	Mole fraction

Greek Letter

α	Water transfer coefficient

ε^{eff}	Effective porosity
ρ	Density, kg/m^3
φ_e	Electrolyte phase potential (varies from -1 to 1), v
μ	Viscosity, kg/ms
σ_m	membrane conductivity, $1/ohm.m$
λ	Water content in the membrane
ζ	Stoichiometric ratio
η	Over potential, v
λ_{eff}	Effective thermal conductivity, w/mk

Subscripts and superscripts

a	Anode
c	Cathode
ch	Channel
k	Chemical species
m	Membrane
MEA	Membrane electrolyte assembly
ref	Reference value
sat	Saturated
w	Water

REFERENCES

[1] William Grubb, Proceedings of the 11th Annual Battery Research and Development Conference, PSC Publications Committee, Red Bank, NJ, p. 5, 1957; *U.S. Patent No. 2,913,511* (1959).

[2] Sandip Dutta, Sirivatch Shimpalee, Justin Van Zee, Three-Dimensional Numerical Simulations of Straight Channel PEM Fuel Cells, *Journal of Applied Electrochemistry*, **30**: 135-146 (2000).

[3] Torsten Berning and Ned Djilali, Three-Dimensional Computational Analysis of Transport Phenomena in a PEM Fuel Cell-a Parametric Study, *J. Power Source*, **124**: 440-452 (2003).

[4] Dewan Hasan Ahmed, Hyung Jin Sung, Effects of Channel Geometrical Configuration and Shoulder width on PEMFC Performance at High Current Density, *Journal of Power Sources,* **162**: 327-339 (2006).

[5] Majidifar S., Mirzaei I., Rezazadeh S., Mohajeri, Hamed Oryani P., Effect of Gas Channel Geometry on Performance of PEM Fuel Cells, *Australian Journal of Basic and Applied Sciences*, **5**: 943-954 (2011).

[6] Pourmahmoud N., Rezazadeh S., Mirzaee I., Heidarpoor V., Three-Dimensional Numerical Analysis of Proton Exchange Membrane Fuel Cell, *Journal of Mechanical Science and Technology (JMST)*, **25** (10): 2665~2673 (2011).

[7] Ahmadi N., Pourmahmoud N,, Mirzaee I., Rezazadeh S., Three-Dimensional Computational Fluid Dynamic Study of Effect of Different Channel and Shoulder Geometries on Cell Performance, *Australian Journal of Basic and Applied Sciences*, **5**(12): 541-556 (2011).

[8] Ahmadi N., Rezazadeh S., Mirzaee I., Pourmahmoud N., Three-Dimensional Computational Fluid Dynamic Analysis of the Conventional PEM Fuel Cell and Investigation of Prominent Gas Diffusion Layers Effect, *Journal of Mechanical Science and Technology JMST*, **26**(8): 1-11 (2012).

[9] Chi Seung Lee, Sung Chul Yi, Numerical Methodology for Proton Exchange Membrane Fuel Cell Simulation Using Computational Fluid Dynamics Technique, *KJCE*, **21**(6): 1153-1160 (2004).

[10] Tae-Hyun Yang, Gu-gon Park, Perumal Pugazhendhi, Won-Yong Lee, Chang Soo Kim, Performance Improvement of Electrode for Polymer Electrolyte Membrane Fuel Cell, *KJCE*, **19**(3): 417-420 (2002).

[11] Golamreza Molaeimanesh, Mohammad Hadi Akbari, Water Droplet Dynamic Behavior During Removal from a Proton Exchange Membrane Fuel Cell Gas Diffusion Layer by Lattice-Boltzmann Method, *KJCE*, **31**(4): 598-610 (2014).

[12] Christophe Carral, Patrice Mélé, A Numerical Analysis of PEMFC Stack Assembly Through a 3D Finite Element Model, *Int. J. Hydrog. Energy.*, **39**(9): 4516-4530 (2014).

[13] Chi Young Jung, Jay Jung Kim, Soo Youn Lim, Sung Chul Yi, Numerical Investigation of the Permeability Level of Ceramic Bipolar Plates for Polymer Electrolyte Fuel Cells, *Journal of Ceramic Processing Research*, **8**(5): 369-375 (2007).

[14] Lin Wang, Attila Husar, Tianhong Zhou, Hongtan Liu, A Parameteric Study of PEM Fuel Cell Performances, *Int. J. Hydrog. Energy*, **28**(11): 1263-1272 (2003).

[15] Ahmadi, Nima, Sajad Rezazadeh, Iraj Mirzaee, Study the Effect of Various Operating Parameters of Proton Exchange Membrane, *Periodica Polytechnica. Chemical Engineering*, **59**(3): 221 (2015).

[16] He, Y., Chen, C., Yu, H., & Lu, G., Effect of Temperature on Compact Layer of Pt Electrode in PEMFCs by First-Principles Molecular Dynamics Calculations, *Applied Surface Science*, **392**: 109-116 (2017).

[17] Yan W.M., Li H.Y., Weng W.C., Transient Mass Transport and Cell Performance of a PEM Fuel Cell, *International Journal of Heat and Mass Transfer,* **107**: 646-656 (2017).

[18] Seddiq, Mehdi, Hassan Khaleghi, Masaud Mirzaei. Parametric Study of Operation and Performance of a PEM Fuel Cell Using Numerical Method, *Iran. J. Chem. Chem. Eng. (IJCCE),* **27**(2): 1-12 (2008).